Sediment transport module

SISYPHE vs. GAIA

History and evolution of novel module

- The module SISYPHE has been developed for more than 30 years (1990-).
- Originally based on the same finite element structure as the two-dimensional code solving the shallow water equations. This shallow water code later evolved into a module that was baptized TELEMAC-2D.
- From early discussions starting 2014, the brand new sediment transport and bed evolution module GAIA of the TMS is introduced.
- GAIA, building upon the SISYPHE module, is able to model complex sediment and morphodynamic processes in coastal areas, rivers, lakes and estuaries, accounting for spatial and temporal variability of sediment size classes (uniform, graded or mixed), properties (cohesive and non-cohesive) and transport modes (suspended, bedload and both simultaneously).

Comparison of SISYPHE and GAIA

- Same aspects:
  - **Solve the Exner equation for sediment mass**
  - Their robustness, flexibility and capability of dealing with a large number of full compatibility between 2D and 3D processes.
- Modified aspects:
  - The GAIA’s generalized framework used for bed layering enables any combination of multiple size classes for both non-cohesive and cohesive sediment to be modelled simultaneously.
  - In contrast to SISYPHE, the quantity of each sediment class in the bed is evaluated using dry mass instead of volume, which minimizes roundoff errors.

Coupled with the modules

Hydrodynamic modules
(TELEMAC-2D or -3D)

Sediment transport module
(GAIA)

Sediment dredging module
(NESTOR)

Wave propagation module
(TOMAWAC)

Water quality module
(WAQTEL.)

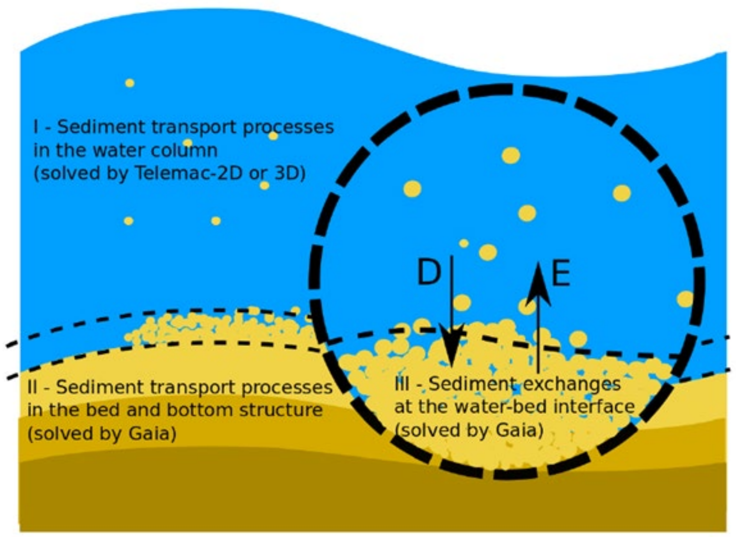

Sketch summarizing the way in which the sediment transport mechanisms are dealt in GAIA. Above, D and E stand for deposition and entrainment fluxes.

Morphodynamic model

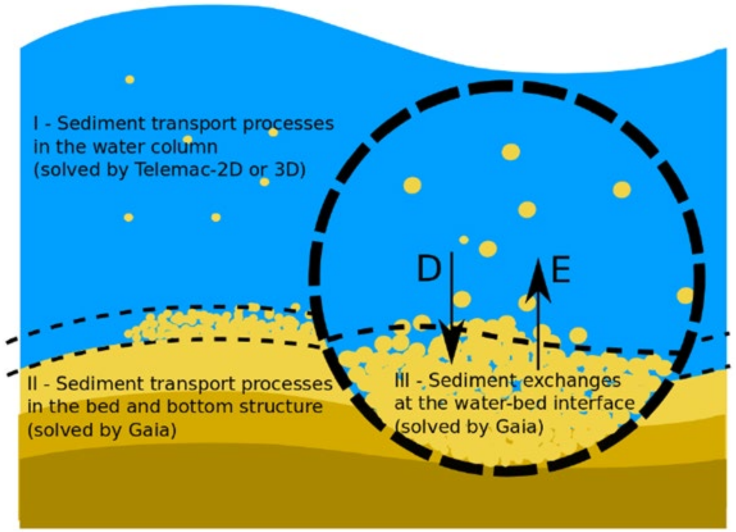

Hydrodynamic → Sediment transport → Bed evolution

Hydrodynamic: Solved conservative laws of mass and momentum

Sediment transport: With predictors for sediment transport capacity

Bed evolution: With conservative law for sediment mass

The main mechanisms of sediment transport are classified as:

- **Bedload**: with a variety of closure relationships for sediment transport capacity.
- **Suspended load**: with the solution of the advection-diffusion equation (ADE) plus closures for erosion and deposition fluxes, equilibrium concentration
- **Bed evolution**: with the solution of the sediment mass conservation equation or Exner equation.

Different types of sediment can be classified as:

- **Non-cohesive**: with equilibrium formulas.
- **Cohesive**: erosion and deposition laws, consolidation models.
- **Mixed-size sediments**: accounting for moderately or poorly sorted sediment distribution, sand-gravel and sand-mud mixtures.

Coupling hydrodynamics to morphodynamics

- **Fully coupled**: respective equations (sediment transport and flow) are coupled and should be solved simultaneously.

[Suitable for hyper-concentrated sediment–laden floods, and debris flow]

- **Decoupled**: Applicable when the typical time scale for river bed adjustment is much longer than the typical time scale for water flow. This procedure, known as asynchronous solution, considers that the bottom is fixed when the flow variables are computed by the hydrodynamics module.

[For the current version of GAIA, the decoupled approach is implemented.]

Currents only

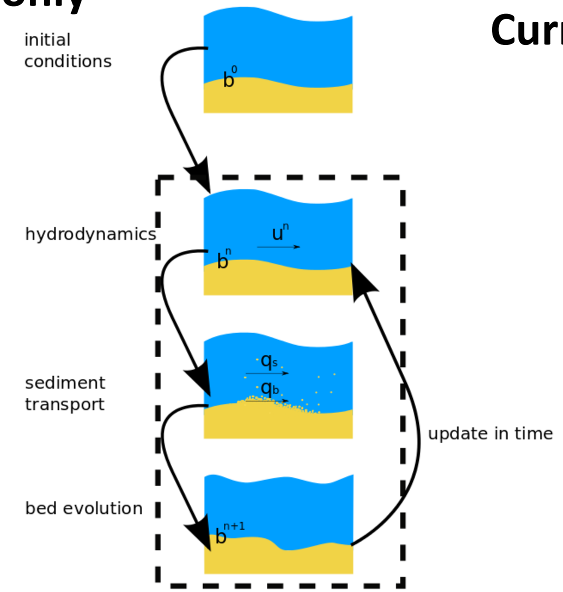

Currents + waves

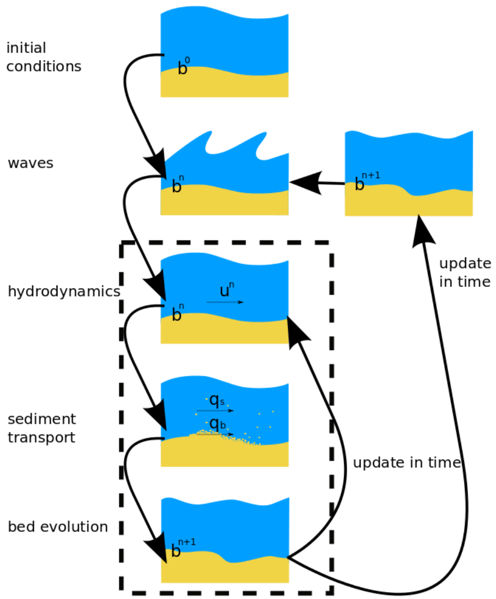

Schematic coupling strategies for GAIA

Sketch of sediment transport in water

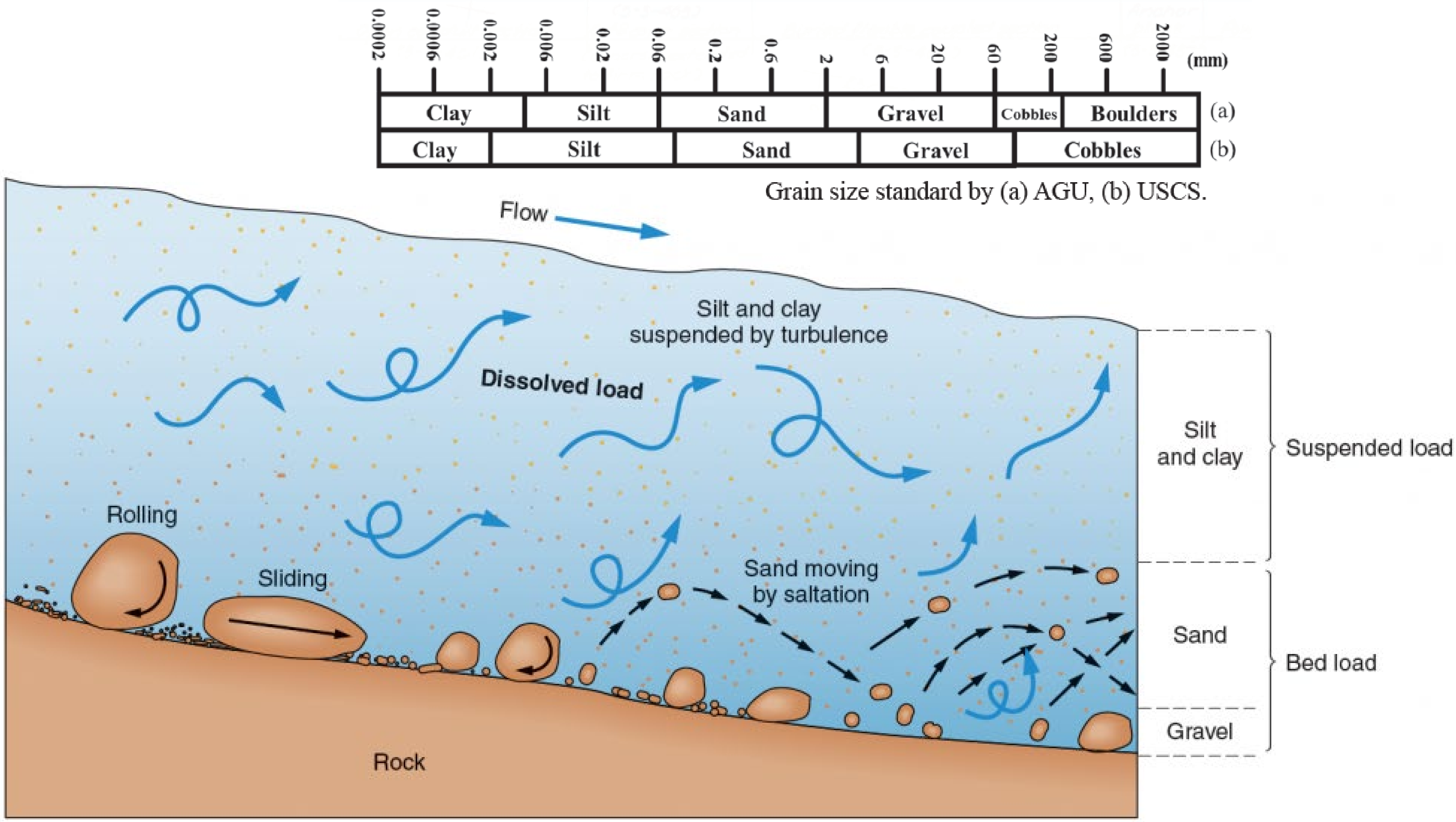

non-cohesive

cohesive

(http://worldrivers.net/2020/03/31/sediment-transport/)

Sediment transport: non-cohesive suspended load

- **Suspended load:** with the solution of the advection-diffusion equation (ADE) plus closures for erosion and deposition fluxes, equilibrium concentration
  - **two-dimensional advection-diffusion equation:**

$$\frac{\partial hC}{\partial t}+\frac{\partial hUC}{\partial x}+\frac{\partial hVC}{\partial y}=\frac{\partial}{\partial x}\left(h\varepsilon_s\frac{\partial C}{\partial x}\right)+\frac{\partial}{\partial y}\left(h\varepsilon_s\frac{\partial C}{\partial y}\right)+E-D$$

where $C=C(x,y,t)$ is the depth-averaged concentration **expressed in g/l**, (U,V) are the depth-averaged components of the velocity in the x and y directions, respectively, ε_s is the turbulent diffusivity of the sediment, often related to the eddy viscosity $\varepsilon_s=\nu_t/\sigma_c$, with σ_c the Schmidt number. In our case, $\sigma_c=1.0$.

  - **three-dimensional advection-diffusion equation:**

$$\frac{\partial C}{\partial t}+\frac{\partial uC}{\partial x}+\frac{\partial vC}{\partial y}+\frac{\partial wC}{\partial z}-\frac{\partial w_sC}{\partial z}=\frac{\partial}{\partial x}\left(\varepsilon_s\frac{\partial C}{\partial x}\right)+\frac{\partial}{\partial y}\left(\varepsilon_s\frac{\partial C}{\partial y}\right)+\frac{\partial}{\partial y}\left(\varepsilon_s\frac{\partial C}{\partial z}\right)$$

where $C=C(x,y,z,t)$ is the concentration **expressed in g/l**, (u,v,w) are the components of the velocity in the x, y and z directions, respectively. w_s is the sediment settling velocity. ε_s is the turbulent diffusivity of the sediment, often related to the eddy viscosity $\varepsilon_s=\nu_t/\sigma_c$, with σ_c the Schmidt number. In our case $\sigma_c=1.0$.

Advection-diffusion equation:

- **Numerical treatment of the diffusion terms:**

The keyword `OPTION FOR THE DIFFUSION OF TRACER` (integer type, set = `1` by default) allows to choose the treatment of the diffusion terms in the advection-diffusion equation 2.1 for the depth-averaged suspended concentration:

- = `1`: the diffusion term is solved in the form $\nabla \cdot (\varepsilon_s \nabla T)$
- = `2`: the diffusion term is solved in the form $\frac{1}{h}\nabla \cdot (h\varepsilon_s \nabla T)$

This keyword must be activated in the steering file of TELEMAC-2D; user can refer to the corresponding user manual for further details.

- **Numerical treatment of the advection terms**

The choice for the scheme for the treatment of the advection terms can be done with the keyword `SCHEME FOR ADVECTION OF SUSPENDED SEDIMENTS` (integer type, set = `5` by default):

```
1="CHARACTERISTICS"
2="SUPG"
3="CONSERVATIVE N-SCHEME"
4="CONSERVATIVE N-SCHEME"
5="CONSERVATIVE PSI-SCHEME"
13="EDGE-BASED N-SCHEME"
14="EDGE-BASED N-SCHEME"
15="ERIA SCHEME"
```

- **Method of characteristics** (`1`)
  - Unconditionally stable and monotonous
  - Diffusive for small time steps, Not conservative
- **Method Streamline Upwind Petrov Galerkin SUPG** (`2`)
  - Based on the Courant number criteria
  - Less diffusive for small time steps, Not conservative
- **Conservative N-scheme (similar to finite volumes)** (`3, 4`)
  - Solves the continuity equation under its conservative form
  - Recommended for correction on convection velocity
  - Courant number limitation (sub-iterations to reduce time step)
- **Edge-based N-scheme NERD** (`13, 14`)
  - Same as `3` and `4` but adapted to tidal flats
  - Based on positive-depth algorithm
- **Distributive schemes PSI** (`5`)
  - fluxes corrected according to the tracer value: relaxation of Courant number criteria, less diffusive than schemes `4, 14` but larger CPU time
  - Should not be applied for tidal flats
- **Eria scheme** (`15`)
  - Works for tidal flats

It is recommended to use the schemes 4 or 14 for a good compromise between accuracy and computational time (specially if tidal flats are present).

Sediment transport: cohesive suspended load

Aggregation of flocs can lead to the formation of macro-flocs larger than 100 µm.

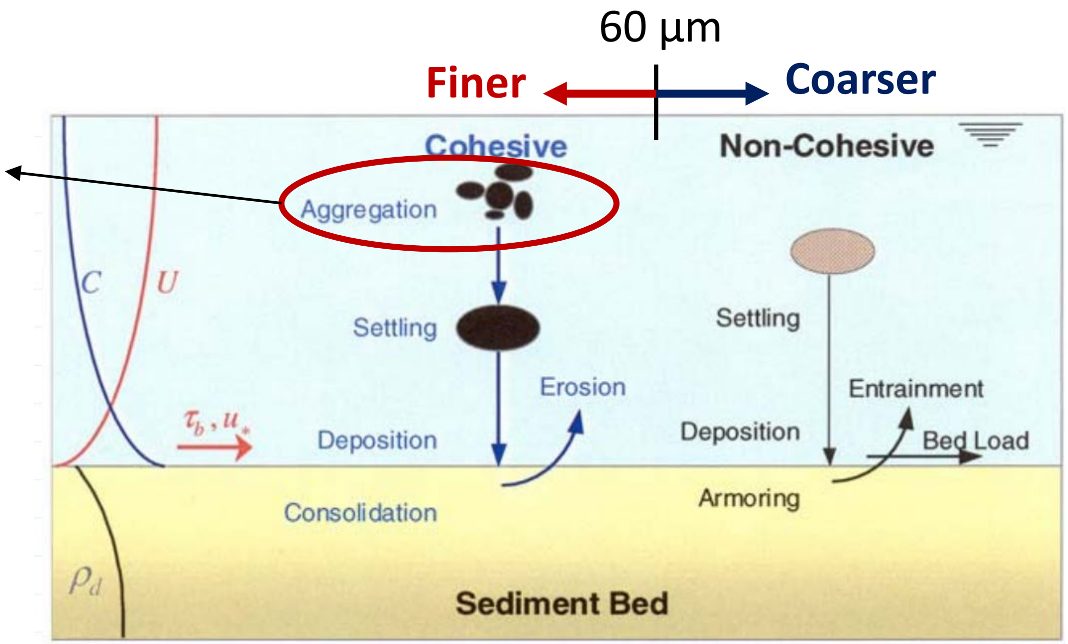

In GAIA, cohesive sediments are accounted by solving the 2D advection-diffusion equation:

$$\frac{\partial hC}{\partial t} + \frac{\partial hUC}{\partial x} + \frac{\partial hVC}{\partial y} = \frac{\partial}{\partial x}\left(h\varepsilon_s \frac{\partial C}{\partial x}\right) + \frac{\partial}{\partial y}\left(h\varepsilon_s \frac{\partial C}{\partial y}\right) + (E - D)$$

$C = C(x,y,t)$ is the depth-averaged concentration expressed in g/l, (U,V) are the depth-averaged components of the velocity in the x and y directions, respectively, ε_s is the turbulent diffusivity of the sediment. Variables E and D are respectively the erosion and deposition fluxes.

Sediment transport: Bedload transport

In contrast to SISYPHE, in GAIA bedload fluxes are computed in terms of (dry) mass transport rate per unit width, without pores.

The dimensionless current-induced sediment transport rate (Φ_b) is expressed:

$$\Phi_b = \frac{Q_b}{\sqrt{g(s-1){D_{50}}^3}}$$

where, Q_b is the bedload transport rate per unit width (m^2/s); $s = \rho_s/\rho_a$ is the relative density; ρ_s and ρ_a is the density of sediment and clear ware (kg/m^3), respectively; D_{50} means sediment grain size (m).

To obtain the sediment transport rate, the bedload transport formulas are commonly computed as the function of Shield number (θ):

$$\theta = \frac{\mu \tau_b}{(\rho_s - \rho_a) g d}$$

where, μ is the skin friction's correction factor.

Solved by bedload transport formula

Keyword `BED-LOAD TRANSPORT FORMULA FOR ALL SANDS` (integer type variable, set to = `1` by default) can be used to set a bedload transport formula. Available formulas in GAIA for bedload transport are:

```
1 : MEYER-PETER and MUELLER
2 : EINSTEIN-BROWN
3 : ENGELUND-HANSEN + CHOLLET ET CUNGE (total sediment transport)
10: WILCOCK AND CROWE
30: ENGELUND-HANSEN (total sediment transport)
7 : VAN RIJN
```

For example, the keyword `BED-LOAD TRANSPORT FORMULA FOR ALL SANDS = 7` sets the van Rijn formula. Please note that bedload transport formulas `3` and `30` account for the total sediment transport.

Sediment Exchanges: Non-cohesive sediment

For non-cohesive sediments, the net sediment flux *E - D* is therefore determined based on the concept of equilibrium concentration: $(E-D)_{z_{ref}} = w_s\left(C_{eq} - C_{z_{ref}}\right)$

The equilibrium near-bed concentration determined by using an empirical formula.

The near-bed concentration, evaluated at the interface between the bed load and the suspended load, $z = z_{ref}$.

Zyserman-Fredsoe

$$C_{eq} = \frac{0.331(\theta' - \theta_{cr})^{1.75}}{1 + 0.72(\theta' - \theta_{cr})^{1.75}},$$

Bijker

$$C_{eq} = \frac{Q_b}{b\, z_{ref}\, u_*}$$

van Rijn

$$C_{eq} = 0.015\, d_{50} \frac{(\theta'/\theta_{cr} - 1)^{3/2}}{z_{ref} D_*^{0.3}}$$

Soulsby & van Rijn

$$C_{eq} = \begin{cases} A_{ss}\left(\sqrt{U_c^2 + \frac{0.018}{C_D} U_w^2} - U_{cr}\right)^{2.4} & \text{if} \geq U_{cr} \\ 0.0 & \text{otherwise} \end{cases}$$

In 2D cases, the near-bed concentration is computed assuming a Rouse profile for the vertical concentration distribution, which is theoretically valid in uniform steady flow conditions:

$$C(z) = C_{z_{ref}} \left(\frac{z-h}{z}\frac{a}{a-h}\right)^R, \tag{4.1}$$

where R is the Rouse number defined by

$$R = \frac{w_s}{\kappa u_*}, \tag{4.2}$$

with κ the von Karman constant ($\kappa = 0.4$), u_* the friction velocity corresponding to the total bed shear stress, and a the reference elevation above the bed elevation. The distance a, defined variously by various authors, is taken to be very close to the bed.
By depth-integration of the Rouse profile (4.3), the following relation can be established between the depth-averaged concentration and the reference concentration (near-bed concentration):

$$C_{z_{ref}} = FC,$$

where:

$$F^{-1} = \left(\frac{z_{ref}}{h}\right)^R \int_{z_{ref}/h}^{1} \left(\frac{1-u}{u}\right)^R du. \tag{4.3}$$

In GAIA, the following expression is used to compute F:

$$F^{-1} = \begin{cases} \frac{1}{(1-Z)} B^R\left(1 - B^{(1-R)}\right) & \text{if} R \neq 1 \\ -B \log B & \text{if} R = 1 \end{cases}$$

with $B = z_{ref}/h$.

Sediment Exchanges: Cohesive and mixed sediment

Erosion flux

The erosion flux is computed with the Partheniades formula. For uniform beds, the erosion flux is related to the excess of applied bed shear stress to the bed shear strength at the bed surface:

$$E = \begin{cases} M\left[\left(\frac{\tau_b}{\tau_{ce}}\right) - 1\right] & \text{if } \tau_b > \tau_{ce} \\ 0 & \text{otherwise} \end{cases}$$

where M the Krone-Partheniades erosion law constant [kg/m^2/s] and τ_{ce} the critical bed shear stress.

The composition of the sediment mixture in the surface (active) layer is taken into consideration when computing the critical shear stress for erosion and the erosion rate. This is achieved by combining the critical shear stresses for erosion for all the sediment classes (cohesive and non-cohesive), according to [30]:

- If the mass of cohesive sediment as a fraction of the mixture is $\geq 50\%$, then the erosion rate and critical shear stress for cohesive sediment alone is used.
- If the mass of cohesive sediment as a fraction of the mixture is $\leq 30\%$, then the erosion rate for non-cohesive sediment is used and the critical shear stress for non-cohesive sediment is used with a correction.
- If the mass of cohesive sediment as fraction of the mixture is $\geq 30\%$ and $\leq 50\%$, then the values are interpolated between the previous values.

Sediment Exchanges: Cohesive and mixed sediment

Deposition flux

The deposition flux for mud is computed by the expression:

$$D = w_s C \left[1 - \left(\frac{\sqrt{\tau_b/\rho}}{u^{cr}_{*mud}} \right)^2 \right]$$

where u^{cr}_{*mud} is the critical shear velocity for mud deposition, expressed in [m/s] and computed as $\sqrt{\tau_{d,mud}/\rho}$ with $\tau_{d,mud}$ provided by the keyword `CLASSES CRITICAL SHEAR STRESS FOR MUD DEPOSITION` (real type, set to = `1000.` N/m^2 by default).

Settling velocity, it can be specified by the user or calculated by the model as a function of grain diameter, keyword **SETTLING VELOCITIES** (real list, =-9 by default).

$$w_s = \begin{cases} \dfrac{(s-1)gd_{50}^2}{18\nu}, & \text{if } d_{50} \leq 10^{-4} \\ \dfrac{10\nu}{d_{50}}\left(\sqrt{1+0.01\dfrac{(s-1)gd_{50}^3}{\nu^2}}-1\right), & \text{if } 10^{-4} \leq d_{50} \leq 10^{-3} \\ 1.1\sqrt{(s-1)gd_{50}}, & \text{otherwise} \end{cases}$$

with $s = \rho_s/\rho_0$ is the relative density and g is the acceleration of the gravity.

Publication: using Gaia for sediment transport simulation

Introducing GAIA, the brand new sediment transport module of the TELEMAC-MASCARET system

Contributors to GAIA *in alphabetical order:* Yoann Audouin[4], Thomas Benson[5], Matthieu Delinares[1], Jacques Fontaine[4], Boris Glander[2], Nicolas Huybrechts[3], Rebekka Kopmann[2], Agnès Leroy[4,6], Sara Pavan[4], Chi-Tuân Pham[4], Florent Taccone[4], Pablo Tassi[4,6,*] & Regis Walther[1]

[1]Artelia; [2]BAW; [3]CEREMA; [4]EDF R&D; [5]HR-Wallingford; [6]Laboratoire d'Hydraulique Saint-Venant

* *Corresponding author:* pablo.tassi@edf.fr

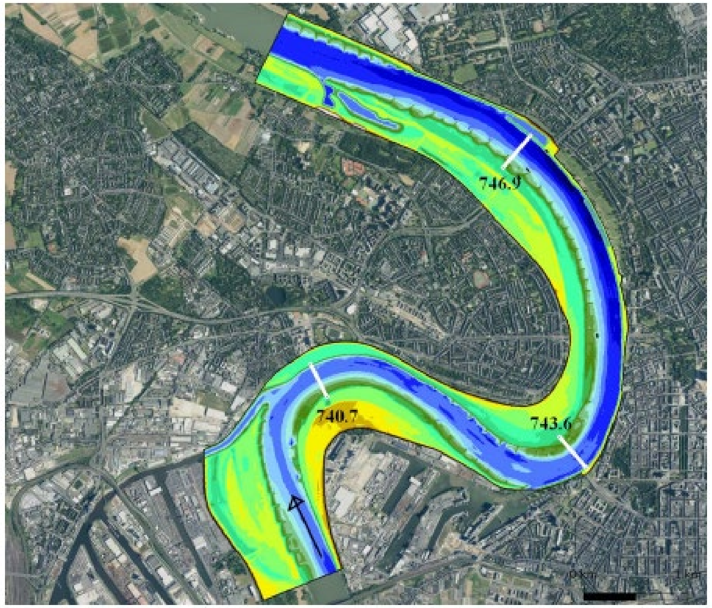

Fig. 5: Lower Rhine river topography and numerical model boundaries nearby Düsseldorf (Germany) (© Bundesamt für Kartographie und Geodäsie (2018)).

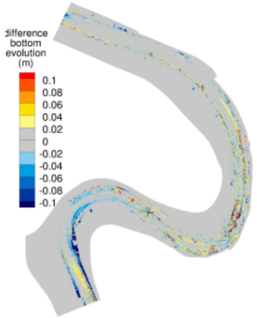

Fig. 7: Differences of the bottom evolution between GAIA and SISYPHE after 6.5 years.

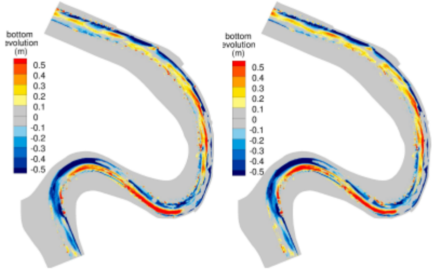

(a) GAIA (b) SISYPHE

Fig. 8: Bottom evolution after 6.5 years

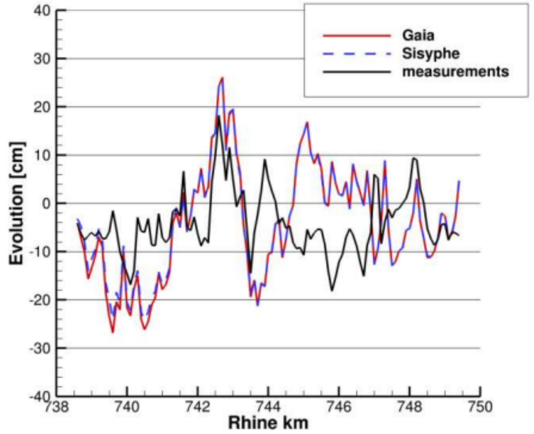

Fig. 6: Comparison of the mean bottom evolution after 6.5 years computed by GAIA and SISYPHE to measurements.

Mass balance	SISYPHE	GAIA
Mass lost (t)	493	655
Initial mass (Mt)	669	669
Relative error to initial mass	0.7×10^{-4}	1×10^{-4}

TABLE I: Comparison of final mass balance between SISYPHE and GAIA.

Publication: using Gaia for sediment transport simulation

Implementation of a novel approach accounting for the influence of vegetation on sediment transport in GAIA

Jiaze Li[1,2,5], Nicolas Claude[3], Pablo Tassi[1,2], Florian Cordier[1], Alessandra Crosato[4], Stéphane Rodrigues[5]
[1] National Hydraulics and Environment Laboratory (LNHE), EDF R&D, Chatou, France
2 Saint-Venant Hydraulics Laboratory (LHSV), ENPC, Cerema, EDF R&D, Chatou, France
3Centre d'Ingénierie Hydraulique, EDF, La Motte Servolex, France
4 Department of Water Resources and Ecosystems, IHE-Delft, Delft, Pays-Bas
5 UMR CNRS 7324 CITERES – Polytech Tours, Tours, France

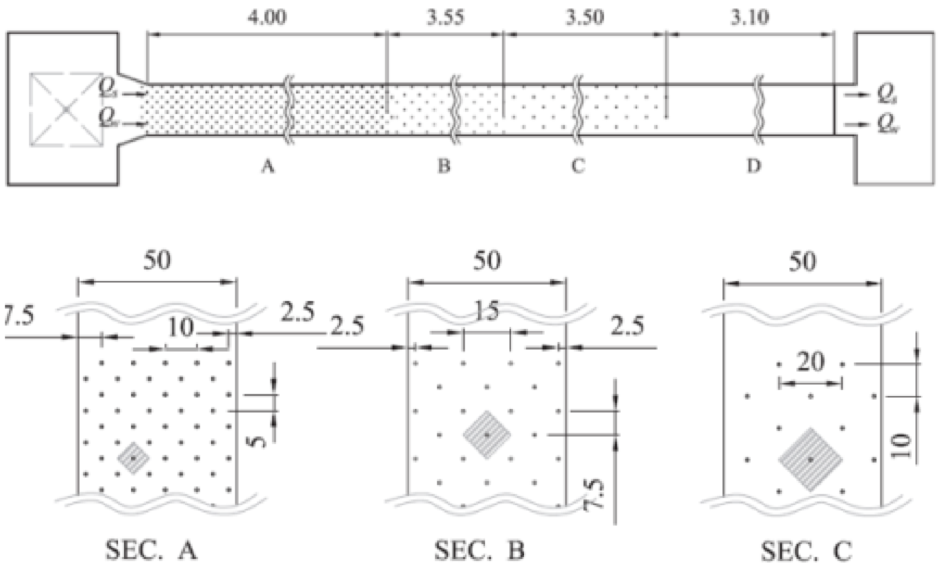

Figure 6: Flume vegetation areas: (A) reach with dense configuration (200 plants/m^2), (B) reach with intermediate density (100 plants/m^2), (C) reach with sparse configuration (50 plants/m^2), D) vegetation-free reach. (reproduced from Armanini & Cavedon (2019) [8])

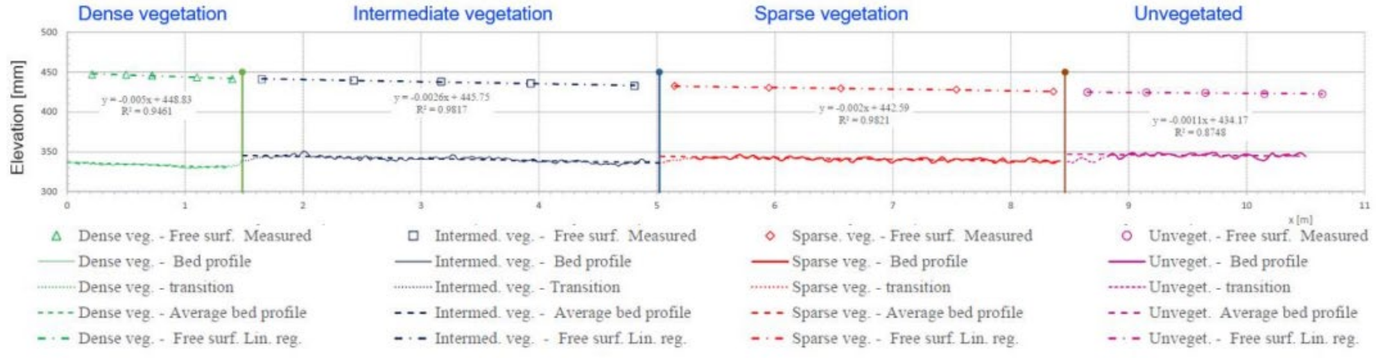

Figure 8: Measured longitudinal profiles of bed elevation and free surface of scenario NP1 (source: Armanini & Cavedon [8])

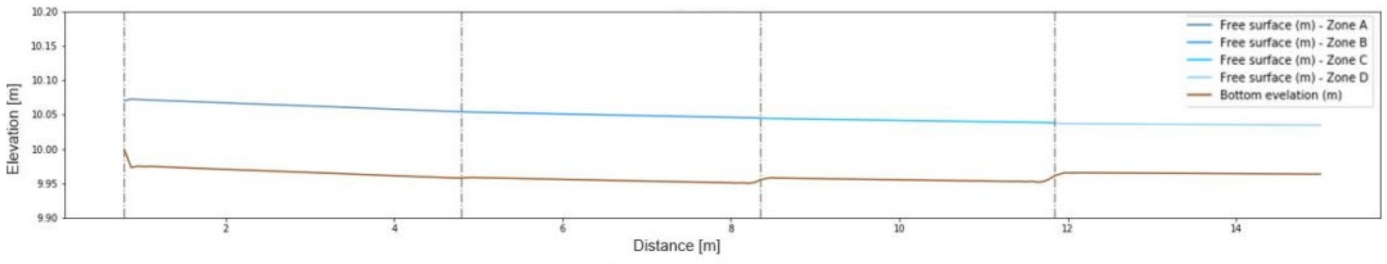

Figure 9: Numerical longitudinal profiles of bed elevation and free surface of scenario NP1 (extracted along y=0.25 m)

Publication: using Gaia for sediment transport simulation

Modelling scour around submerged objects with TELEMAC3D - GAIA

Irinios Yiannoukos
School of Ocean Sciences
Bangor University
Bangor, UK
i.yiannoukos@bangor.ac.uk

Katrien Van Landeghem; Michael Roberts; Barney Smyth; Jacob Morgan
Bangor University, Bangor, UK
Amelia Couldrey; Thomas Benson; Richard Whitehouse; Connor McCarron
HR Wallingford, Wallingford, UK
Rory Quinn
Ulster University, Coleraine, UK

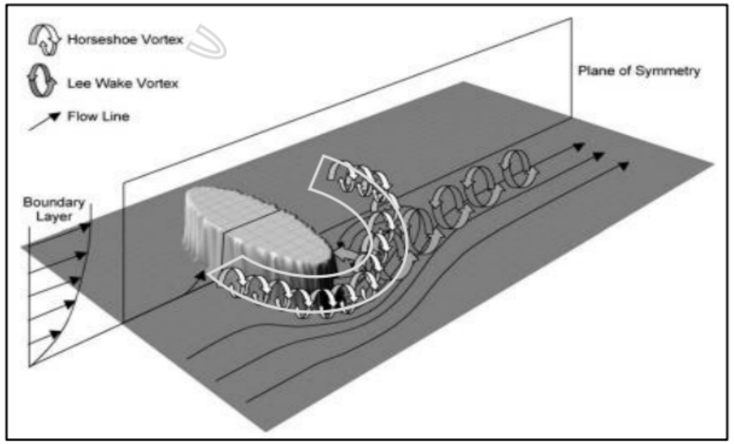

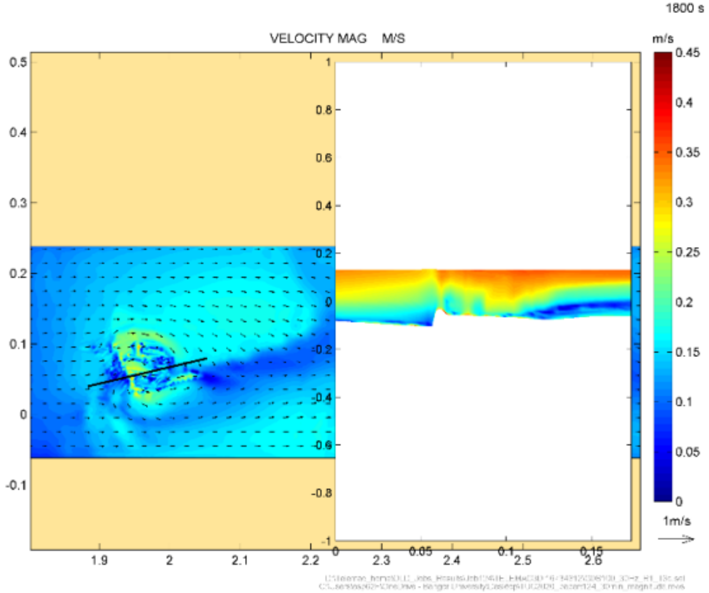

Figure 6: Magnitude of the flow after 30 minutes of simulation taken at the first horizontal plane above the bed (j=2)

Measurement

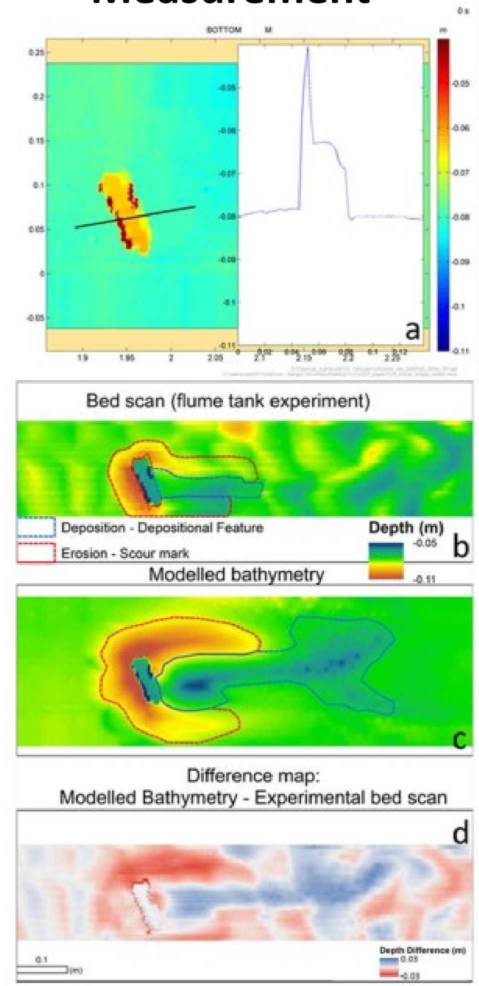

Figure 7: Profile showing the shape of the object as captured by the 3D SeaTek bed scan transducers (7a) Experimental bed scan (7b) compared th Modelled bathymetry (7c) and Difference map of the modelled and the experimental bathymetry (7d).

Simulation

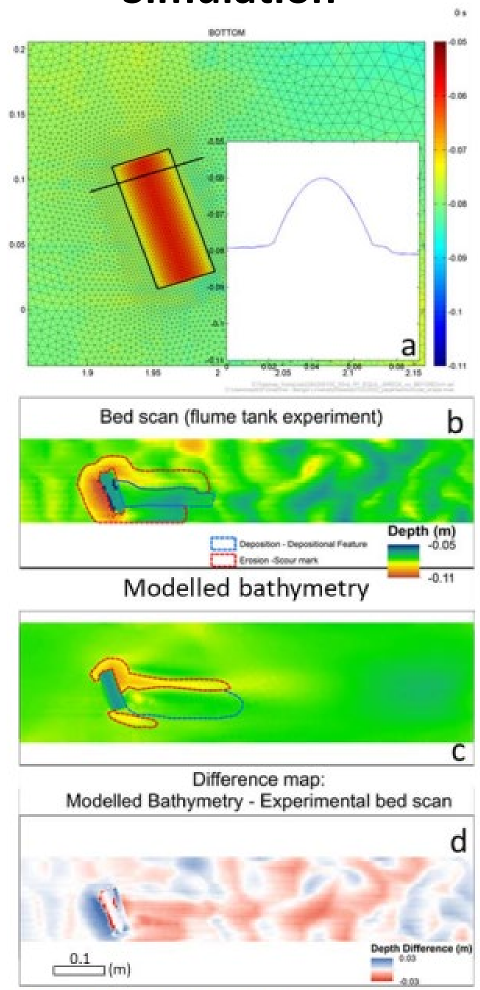

Figure 8: a) 2D representation of the half-cylinder in the computation domain (profile created from the horizontal line in the middle of the object) and representation of the geometry (mesh) of the computation domain around the object 8b) Experimental bed scan 8c) Modelled bathymetry and 8d) Difference map of the difference between the modelled and the experimental data.

Publication: using Gaia for sediment transport simulation

Simulation of embayment lab experiments with TELEMAC-2D/GAIA

Rebekka Kopmann
Hydraulic Engineering in Inland Areas
Federal Waterways Engineering and Research Institute (BAW)
Karlsruhe, Germany
Rebekka.kopmann@baw.de

Javier Perez Obreque
Institute for Water and River Basin
Karlsruhe Institute of Technology
Karlsruhe, Germany

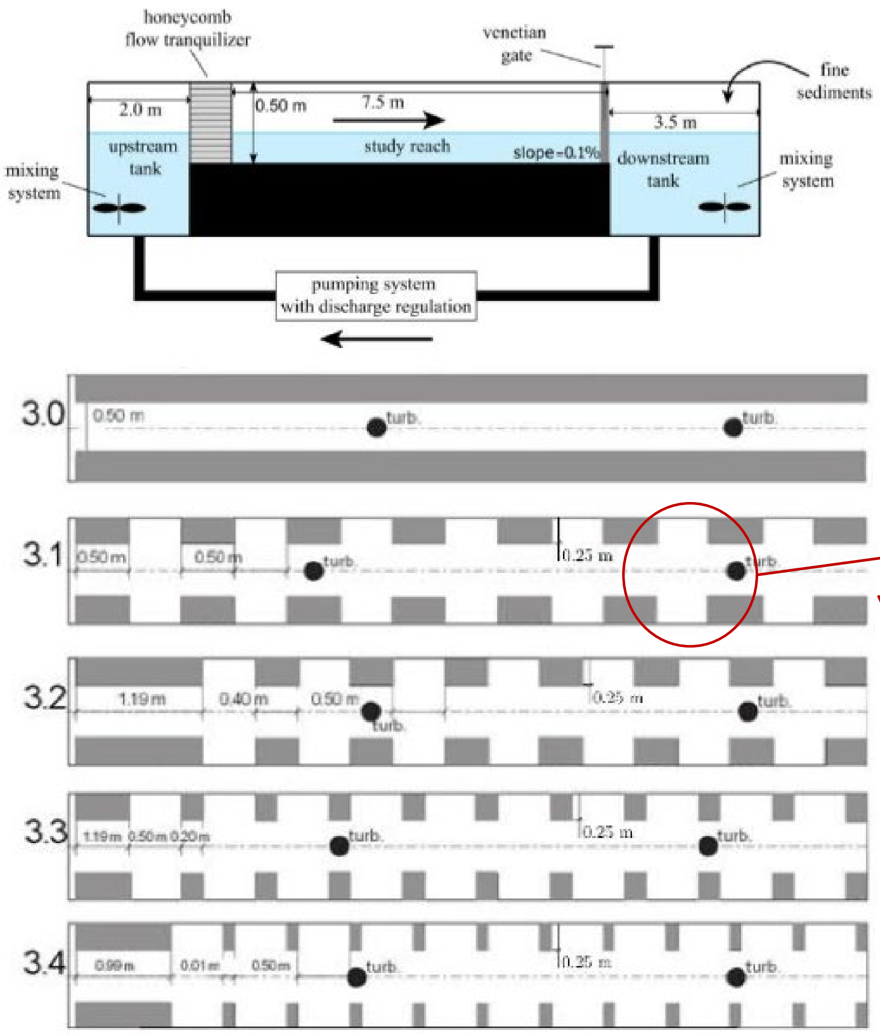

Figure 1: Side view of the set-up of the flume experiment (top) and topview on embayment configurations group 3 (bottom) (from [1]).

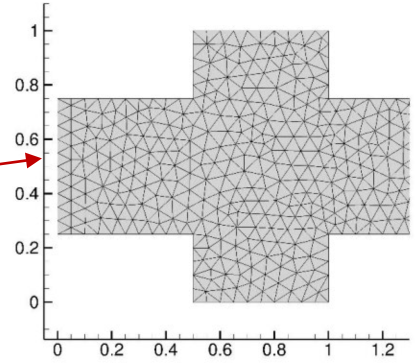

Figure 3: Part of the simulation grid for embayment configuration 3.1.

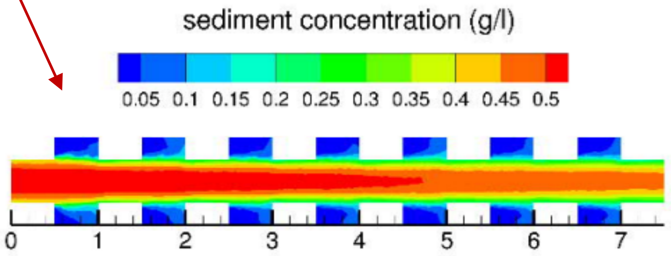

Figure 4: Initial concentration from a previous steady state simulation for embayment configuration 3.1 and the discharge 4.8 l/s.

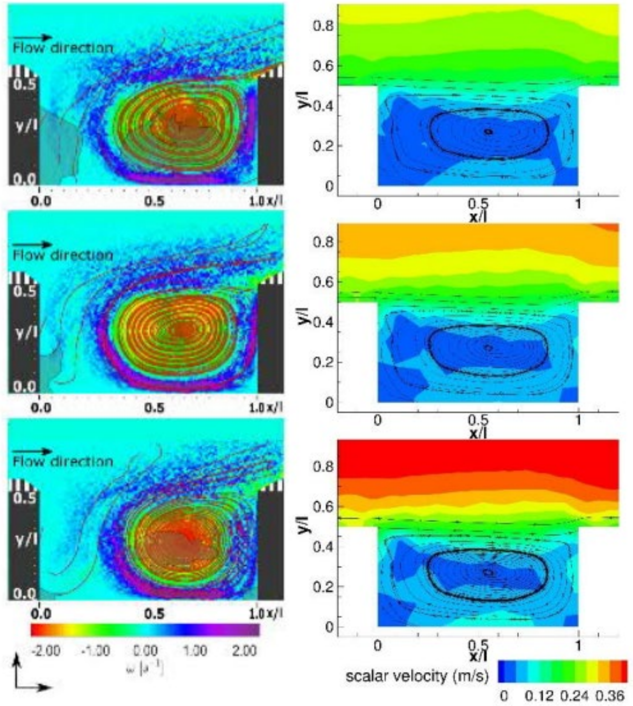

Figure 5: Comparison of measured vorticity and streamlines of the groyne gyre (left, from supplementary online data of [1]) and simulated scalar velocity and streamlines of the groyne gyre (right) for low (top), medium (middle) and high (bottom) discharges for configuration 3.1.